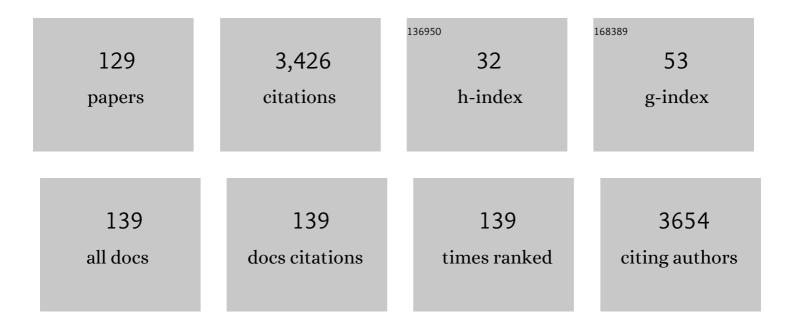
List of Publications by Year in descending order

Source: https://exaly.com/author-pdf/9054763/publications.pdf Version: 2024-02-01



ACATA A FYNED

#	Article	IF	CITATIONS
1	Agarose gel stiffness determines rate of DRG neurite extension in 3D cultures. Biomaterials, 2001, 22, 1077-1084.	11.4	470
2	Formulation and Characterization of Echogenic Lipidâ^'Pluronic Nanobubbles. Molecular Pharmaceutics, 2010, 7, 49-59.	4.6	117
3	Acoustic Characterization and Pharmacokinetic Analyses of New Nanobubble Ultrasound Contrast Agents. Ultrasound in Medicine and Biology, 2013, 39, 2137-2146.	1.5	117
4	Ultrasound molecular imaging of ovarian cancer with CA-125 targeted nanobubble contrast agents. Nanomedicine: Nanotechnology, Biology, and Medicine, 2017, 13, 2159-2168.	3.3	102
5	Effect of injection site on in situ implant formation and drug release in vivo. Journal of Controlled Release, 2010, 147, 350-358.	9.9	92
6	Contrast enhanced ultrasound imaging by nature-inspired ultrastable echogenic nanobubbles. Nanoscale, 2019, 11, 15647-15658.	5.6	86
7	Ultrasound imaging beyond the vasculature with new generation contrast agents. Wiley Interdisciplinary Reviews: Nanomedicine and Nanobiotechnology, 2015, 7, 593-608.	6.1	79
8	Improving performance of nanoscale ultrasound contrast agents using N,N-diethylacrylamide stabilization. Nanomedicine: Nanotechnology, Biology, and Medicine, 2017, 13, 59-67.	3.3	79
9	Enhancement of carboplatin toxicity by Pluronic block copolymers. Journal of Controlled Release, 2005, 106, 188-197.	9.9	77
10	Characterization of different bubble formulations for blood-brain barrier opening using a focused ultrasound system with acoustic feedback control. Scientific Reports, 2018, 8, 7986.	3.3	71
11	Ultrasound Contrast Agents and Delivery Systems in Cancer Detection and Therapy. Advances in Cancer Research, 2018, 139, 57-84.	5.0	67
12	Noninvasive characterization of in situ forming implants using diagnostic ultrasound. Journal of Controlled Release, 2010, 143, 183-190.	9.9	65
13	Sink or float? Characterization of shell-stabilized bulk nanobubbles using a resonant mass measurement technique. Nanoscale, 2019, 11, 851-855.	5.6	62
14	PMMA-Fe ₃ O ₄ for internal mechanical support and magnetic thermal ablation of bone tumors. Theranostics, 2019, 9, 4192-4207.	10.0	62
15	Time-intensity-curve Analysis and Tumor Extravasation of Nanobubble Ultrasound Contrast Agents. Ultrasound in Medicine and Biology, 2019, 45, 2502-2514.	1.5	60
16	MultimodalIn VivoImaging Exposes the Voyage of Nanoparticles in Tumor Microcirculation. ACS Nano, 2013, 7, 3118-3129.	14.6	59
17	Drug-eluting polymer implants in cancer therapy. Expert Opinion on Drug Delivery, 2008, 5, 775-788.	5.0	52
18	Nanobubble Ultrasound Contrast Agents for Enhanced Delivery of Thermal Sensitizer to Tumors Undergoing Radiofrequency Ablation. Pharmaceutical Research, 2014, 31, 1407-1417.	3.5	52

#	Article	IF	CITATIONS
19	Cryo-EM Visualization of Lipid and Polymer-Stabilized Perfluorocarbon Gas Nanobubbles - A Step Towards Nanobubble Mediated Drug Delivery. Scientific Reports, 2017, 7, 13517.	3.3	52
20	Role of Surface Tension in Gas Nanobubble Stability Under Ultrasound. ACS Applied Materials & Interfaces, 2018, 10, 9949-9956.	8.0	52
21	Enhancing Tumor Drug Distribution With Ultrasound-Triggered Nanobubbles. Journal of Pharmaceutical Sciences, 2019, 108, 3091-3098.	3.3	52
22	Modeling doxorubicin transport to improve intratumoral drug delivery to RF ablated tumors. Journal of Controlled Release, 2007, 124, 11-19.	9.9	51
23	Noninvasive Characterization of the Effect of Varying PLGA Molecular Weight Blends on <i>In Situ</i> Forming Implant Behavior Using Ultrasound Imaging. Theranostics, 2012, 2, 1064-1077.	10.0	50
24	Effect of Bubble Concentration on the in Vitro and in Vivo Performance of Highly Stable Lipid Shell-Stabilized Micro- and Nanoscale Ultrasound Contrast Agents. Langmuir, 2019, 35, 10192-10202.	3.5	48
25	Real-time Monitoring of Radiofrequency Ablation and Postablation Assessment: Accuracy of Contrast-enhanced US in Experimental Rat Liver Model. Radiology, 2014, 270, 107-116.	7.3	47
26	Bursting microbubbles: How nanobubble contrast agents can enable the future of medical ultrasound molecular imaging and image-guided therapy. Current Opinion in Colloid and Interface Science, 2021, 54, 101463.	7.4	45
27	Characterization of formulation parameters affecting low molecular weight drug release from <i>in situ</i> forming drug delivery systems. Journal of Biomedical Materials Research - Part A, 2010, 94A, 476-484.	4.0	43
28	Toward Precisely Controllable Acoustic Response of Shell-Stabilized Nanobubbles: High Yield and Narrow Dispersity. ACS Nano, 2021, 15, 4901-4915.	14.6	43
29	Real time ultrasound molecular imaging of prostate cancer with PSMA-targeted nanobubbles. Nanomedicine: Nanotechnology, Biology, and Medicine, 2020, 28, 102213.	3.3	41
30	Contrast-enhanced ultrasound with sub-micron sized contrast agents detects insulitis in mouse models of type1 diabetes. Nature Communications, 2020, 11, 2238.	12.8	37
31	Porphyrin-Loaded Pluronic Nanobubbles: A New US-Activated Agent for Future Theranostic Applications. Bioconjugate Chemistry, 2018, 29, 234-240.	3.6	36
32	Biodegradable cascade nanocatalysts enable tumor-microenvironment remodeling for controllable CO release and targeted/synergistic cancer nanotherapy. Biomaterials, 2021, 276, 121001.	11.4	35
33	Biomedical Imaging in Implantable Drug Delivery Systems. Current Drug Targets, 2015, 16, 672-682.	2.1	33
34	Combined radiofrequency ablation and doxorubicin-eluting polymer implants for liver cancer treatment. Journal of Biomedical Materials Research - Part A, 2007, 81A, 205-213.	4.0	31
35	Effect of cargo properties on in situ forming implant behavior determined by noninvasive ultrasound imaging. Drug Delivery and Translational Research, 2012, 2, 45-55.	5.8	30
36	Combined Tumor Therapy by Using Radiofrequency Ablation and 5-FU–Laden Polymer Implants: Evaluation in Rats and Rabbits. Radiology, 2005, 237, 911-918.	7.3	29

#	Article	IF	CITATIONS
37	Inhibition of metastasis by HEXIM1 through effects on cell invasion and angiogenesis. Oncogene, 2013, 32, 3829-3839.	5.9	29
38	Effect of the Subcutaneous Environment on Phase-Sensitive In Situ-Forming Implant Drug Release, Degradation, and Microstructure. Journal of Pharmaceutical Sciences, 2015, 104, 4322-4328.	3.3	29
39	Concurrent visual and acoustic tracking of passive and active delivery of nanobubbles to tumors. Theranostics, 2020, 10, 11690-11706.	10.0	29
40	Macroporous acrylamide phantoms improve prediction of in vivo performance of in situ forming implants. Journal of Controlled Release, 2016, 243, 225-231.	9.9	27
41	Theoretical and Experimental Gas Volume Quantification of Micro- and Nanobubble Ultrasound Contrast Agents. Pharmaceutics, 2020, 12, 208.	4.5	27
42	Combined modeling and experimental approach for the development of dual-release polymer millirods. Journal of Controlled Release, 2002, 83, 427-435.	9.9	25
43	Noninvasive Monitoring of Local Drug Release Using X-ray Ccomputed Tomography: Optimization and In Vitro/In Vivo Validation. Journal of Pharmaceutical Sciences, 2003, 92, 289-296.	3.3	25
44	Injectable Polymer Depot Combined With Radiofrequency Ablation for Treatment of Experimental Carcinoma in Rat. Investigative Radiology, 2006, 41, 890-897.	6.2	25
45	The Effect of Additives on the Behavior of Phase Sensitive In Situ Forming Implants. Journal of Pharmaceutical Sciences, 2015, 104, 3471-3480.	3.3	24
46	Influence of Nanobubble Concentration on Blood–Brain Barrier Opening Using Focused Ultrasound Under Real-Time Acoustic Feedback Control. Ultrasound in Medicine and Biology, 2019, 45, 2174-2187.	1.5	24
47	Advances in image-guided intratumoral drug delivery techniques. Therapeutic Delivery, 2010, 1, 307-322.	2.2	23
48	Structural parameters governing activity of Pluronic triblock copolymers in hyperthermia cancer therapy. International Journal of Hyperthermia, 2011, 27, 663-671.	2.5	23
49	Model simulation and experimental validation of intratumoral chemotherapy using multiple polymer implants. Medical and Biological Engineering and Computing, 2008, 46, 1039-1049.	2.8	22
50	Dual-Targeted Microbubbles Specific to Integrin αVβ3 and Vascular Endothelial Growth Factor Receptor 2 for Ultrasonography Evaluation of Tumor Angiogenesis. Ultrasound in Medicine and Biology, 2018, 44, 1460-1467.	1.5	21
51	Inhibition of the histone demethylase, KDM5B, directly induces re-expression of tumor suppressor protein HEXIM1 in cancer cells. Breast Cancer Research, 2019, 21, 138.	5.0	20
52	Microfluidic Generation of Monodisperse Nanobubbles by Selective Gas Dissolution. Small, 2021, 17, e2100345.	10.0	20
53	Pickering Bubbles as Dual-Modality Ultrasound and Photoacoustic Contrast Agents. ACS Applied Materials & Interfaces, 2020, 12, 22308-22317.	8.0	19
54	Time and Dose Dependence of Pluronic Bioactivity in Hyperthermia-Induced Tumor Cell Death. Experimental Biology and Medicine, 2009, 234, 95-104.	2.4	18

#	Article	IF	CITATIONS
55	Dynamic Evolutionary Changes in Blood Flow Measured by MDCT in a Hepatic VX2 Tumor Implant over an Extended 28-day Growth Period: Time-Density Curve Analysis. Academic Radiology, 2009, 16, 1483-1492.	2.5	18
56	Increasing Doxorubicin Loading in Lipid-Shelled Perfluoropropane Nanobubbles via a Simple Deprotonation Strategy. Frontiers in Pharmacology, 2020, 11, 644.	3.5	18
57	Molecular imaging of orthotopic prostate cancer with nanobubble ultrasound contrast agents targeted to PSMA. Scientific Reports, 2021, 11, 4726.	3.3	18
58	Combination of Sensitizing Pretreatment and Radiofrequency Tumor Ablation: Evaluation in Rat Model. Radiology, 2008, 246, 796-803.	7.3	17
59	Electrospinning and Imaging. Advanced Engineering Materials, 2012, 14, B266.	3.5	17
60	Photoacoustic imaging biomarkers for monitoring biophysical changes during nanobubble-mediated radiation treatment. Photoacoustics, 2020, 20, 100201.	7.8	16
61	Noninvasive monitoring of local drug release in a rabbit radiofrequency (RF) ablation model using X-ray computed tomography. Journal of Controlled Release, 2002, 83, 415-425.	9.9	15
62	Acoustic Actuation of Integrinâ€Bound Microbubbles for Mechanical Phenotyping during Differentiation and Morphogenesis of Human Embryonic Stem Cells. Small, 2018, 14, e1803137.	10.0	15
63	X-ray computed tomography methods for in vivo evaluation of local drug release systems. IEEE Transactions on Medical Imaging, 2002, 21, 1310-1316.	8.9	14
64	Ultrasound-Based Molecular Imaging of Tumors with PTPmu Biomarker-Targeted Nanobubble Contrast Agents. International Journal of Molecular Sciences, 2021, 22, 1983.	4.1	14
65	Effect of intratumoral injection of carboplatin combined with pluronic P85 or L61 on experimental colorectal carcinoma in rats. Experimental Biology and Medicine, 2007, 232, 950-7.	2.4	14
66	Vasomodulation of Tumor Blood Flow: Effect on Perfusion and Thermal Ablation Size. Annals of Biomedical Engineering, 2009, 37, 552-564.	2.5	13
67	Differentiation of Benign Periablational Enhancement from Residual Tumor Following Radio-Frequency Ablation Using Contrast-Enhanced Ultrasonography in a Rat Subcutaneous Colon Cancer Model. Ultrasound in Medicine and Biology, 2012, 38, 443-453.	1.5	13
68	Ultrasound-guided intratumoral delivery of doxorubicin from <i>in situ</i> forming implants in a hepatocellular carcinoma model. Therapeutic Delivery, 2016, 7, 201-212.	2.2	13
69	Radiofrequency Ablation. Academic Radiology, 2009, 16, 321-331.	2.5	11
70	Role of Pluronic block copolymers in modulation of heat shock protein 70 expression. International Journal of Hyperthermia, 2011, 27, 672-681.	2.5	11
71	Increasing Distribution of Drugs Released from In Situ Forming PLGA Implants Using Therapeutic Ultrasound. Annals of Biomedical Engineering, 2017, 45, 2879-2887.	2.5	11
72	Nanobubble Extravasation in Prostate Tumors Imaged with Ultrasound: Role of Active versus Passive Targeting. , 2018, , .		11

5

#	Article	IF	CITATIONS
73	An artificially engineered "tumor bio-magnet―for collecting blood-circulating nanoparticles and magnetic hyperthermia. Biomaterials Science, 2019, 7, 1815-1824.	5.4	10
74	Intracellular vesicle entrapment of nanobubble ultrasound contrast agents targeted to PSMA promotes prolonged enhancement and stability <i>in vivo</i> and <i>in vitro</i> . Nanotheranostics, 2022, 6, 270-285.	5.2	10
75	Induction of HEXIM1 activities by HMBA derivative 4a1: Functional consequences and mechanism. Cancer Letters, 2016, 379, 60-69.	7.2	9
76	In situ forming implants exposed to ultrasound enhance therapeutic efficacy in subcutaneous murine tumors. Journal of Controlled Release, 2020, 324, 146-155.	9.9	9
77	Extrusion: A New Method for Rapid Formulation of High‥ield, Monodisperse Nanobubbles. Small, 2022, 18, e2200810.	10.0	9
78	Nondestructive Characterization of Biodegradable Polymer Erosion in Vivo Using Ultrasound Elastography Imaging. ACS Biomaterials Science and Engineering, 2016, 2, 1005-1012.	5.2	8
79	The dance of the nanobubbles: detecting acoustic backscatter from sub-micron bubbles using ultra-high frequency acoustic microscopy. Nanoscale, 2020, 12, 21420-21428.	5.6	8
80	A feasibility study of high intensity focused ultrasound for liver biopsy hemostasis. Ultrasound in Medicine and Biology, 2004, 30, 1531-1537.	1.5	7
81	Quantitative computed tomography analysis of local chemotherapy in liver tissue after radiofrequency ablation1. Academic Radiology, 2004, 11, 1326-1336.	2.5	7
82	Semiquantitative imaging measurement of baseline and vasomodulated normal prostatic blood flow using sildenafil. International Journal of Impotence Research, 2007, 19, 110-113.	1.8	7
83	Preclinical evaluation of radiosensitizing activity of Pluronic block copolymers. International Journal of Radiation Biology, 2013, 89, 801-812.	1.8	7
84	Validation of Ultrasound Elastography Imaging for Nondestructive Characterization of Stiffer Biomaterials. Annals of Biomedical Engineering, 2016, 44, 1515-1523.	2.5	7
85	Iridium(III) Complex-Loaded Perfluoropropane Nanobubbles for Enhanced Sonodynamic Therapy. Bioconjugate Chemistry, 2022, 33, 1057-1068.	3.6	7
86	Image-Guided Therapeutics. Molecular Pharmaceutics, 2010, 7, 1-2.	4.6	6
87	Development of a High-Throughput Ultrasound Technique for the Analysis of Tissue Engineering Constructs. Annals of Biomedical Engineering, 2016, 44, 793-802.	2.5	6
88	Predicting in vivo behavior of injectable, in situ-forming drug-delivery systems. Therapeutic Delivery, 2017, 8, 479-483.	2.2	6
89	Improving Treatment Efficacy of In Situ Forming Implants via Concurrent Delivery of Chemotherapeutic and Chemosensitizer. Scientific Reports, 2020, 10, 6587.	3.3	6
90	Polymer Nanosheet Containing Star‣ike Copolymers: A Novel Scalable Controlled Release System. Small, 2018, 14, e1800115.	10.0	5

#	Article	lF	CITATIONS
91	Development of a novel castrationâ€resistant orthotopic prostate cancer model in New Zealand White rabbit. Prostate, 2022, 82, 695-705.	2.3	5
92	Efficiency of combined blocking of aerobic and glycolytic metabolism pathways in treatment of N1-S1 hepatocellular carcinoma in a rat model. Journal of Cancer Research and Therapeutics, 2017, 13, 533-537.	0.9	5
93	0079: Direct Measurement of Blood Flow Velocity in Small Diameter Vessels Using Contrast-Enhanced Ultrasound. Ultrasound in Medicine and Biology, 2009, 35, S16.	1.5	4
94	Ultrasound signal from sub-micron lipid-coated bubbles. , 2017, , .		4
95	The Effect of Lipid Solubilization on the Performance of Doxorubicin-Loaded Nanobubbles. , 2018, , .		4
96	Radiofrequency Ablation: Effect of Tumor- and Organ-specific Pharmacologic Modulation of Arterial and Portal Venous Blood Flow on Coagulation Diameter in an N1-S1 Tumor Model. Journal of Vascular and Interventional Radiology, 2012, 23, 826-832.	0.5	3
97	Notice of Removal: On the fate of mesh-stabilized lipid nanobubbles after destruction with ultrasound. , 2017, , .		3
98	High-Frequency Array-Based Nanobubble Nonlinear Imaging in a Phantom and <i>In Vivo</i> . IEEE Transactions on Ultrasonics, Ferroelectrics, and Frequency Control, 2021, 68, 2059-2074.	3.0	3
99	Research Spotlight: Applications of ultrasound for image-guided drug delivery in cancer chemotherapy. Therapeutic Delivery, 2013, 4, 785-789.	2.2	2
100	Theoretical and experimental investigation of the nonlinear dynamics of nanobubbles excited at clinically relevant ultrasound frequencies and pressures: The role of lipid shell buckling. , 2017, , .		2
101	Effect of the surfactant pluronic on the stability of lipid-stabilized perfluorocarbon nanobubbles. , 2017, , .		2
102	Ultrasound-Enhanced Distribution and Treatment Efficacy of Dox-Loaded Intratumoral In Situ Forming Implants in Murine HCT-15 Tumors. , 2018, , .		2
103	The Effect of Freeze/Thawing on the Physical Properties and Acoustic Performance of Perfluoropropane Nanobubble Suspensions. , 2019, , .		2
104	Ultrasound Triggered Drug Release from Affinity-Based β-Cyclodextrin Polymers for Infection Control. Annals of Biomedical Engineering, 2021, 49, 2513-2521.	2.5	2
105	Formulation of a Thermosensitive Imaging Hydrogel for Topical Application and Rapid Visualization of Tumor Margins in the Surgical Cavity. Cancers, 2022, 14, 3459.	3.7	2
106	Image-Guided Development of Biomaterials: Enabling Technologies Shaping and Expediting the Future of Materials in Medicine. Annals of Biomedical Engineering, 2016, 44, 619-620.	2.5	1
107	Ultrasound signal from sub-micron lipid-coated bubbles. , 2017, , .		1
108	Enhancing fluorescein distribution from in situ forming PLGA implants using therapeutic ultrasound. , 2017, , .		1

#	Article	IF	CITATIONS
109	Using ultrasound and photoacoustics to monitor in situ forming implant structure and drug release. , 2017, , .		1
110	Theoretical and experimental investigation of the nonlinear dynamics of nanobubbles excited at clinically relevant ultrasound frequencies and pressures: The role oflipid shell buckling. , 2017, , .		1
111	Nanobubble Facilitated Optoporation and Photoacoustic Imaging of BT-474 Breast Cancer Cells. , 2018, , .		1
112	Quantification of PSMA expression in prostate cancer by pharmacokinetic modeling of targeted ultrasound nanobubbles. , 2019, , .		1
113	In vitro Preparation and Characterization of Magnetic Nanobubbles. , 2019, , .		1
114	Delayed response to proton beam treatment of hepatocellular carcinoma. BJR case Reports, 2020, 6, 20180125.	0.2	1
115	Abstract 260: Apigenin nanoparticle suppresses sphere formation in CD133+/ALDH1highprostate cancer stem cells through downregulation of stem cell markers. , 2018, , .		1
116	Pharmacokinetic Modeling of the Second-Wave Phenomenon in Nanobubble-Based Contrast-Enhanced Ultrasound. IEEE Transactions on Biomedical Engineering, 2023, 70, 42-54.	4.2	1
117	Sonotheranostics and Sonogenetics Special Issue. Bioconjugate Chemistry, 2022, 33, 991-992.	3.6	1
118	Enhancing fluorescein release from in-situ forming PLGA implants using therapeutic ultrasound. , 2017, , .		0
119	Ultrasound characterization of slow precipitating implants for vascular occlusion. , 2017, , .		Ο
120	Notice of Removal: Nanobubble contrast agents enhance ultrasound imaging of prostate tumors in mice. , 2017, , .		0
121	Effect of the surfactant pluronic on the stability of lipid-stabilized perfluorocarbon nanobubbles. , 2017, , .		Ο
122	Using ultrasound and photoacoustics to monitor in situ forming implant structure and drug release. , 2017, , .		0
123	Ultrasound characterization of slow precipitating implants for vascular occlusion. , 2017, , .		Ο
124	Tunable Polymer Embolic Implant for Vascular Occlusion. ACS Biomaterials Science and Engineering, 2019, 5, 1849-1856.	5.2	0
125	Radiation-enhanced nanobubble therapy: Monitoring treatment effects using photoacoustic imaging. , 2019, , .		0
126	TECHNIQUES IN X-RAY COMPUTED TOMOGRAPHY IN THE EVALUATION OF DRUG RELEASE SYSTEMS AND		0

^o THEIR APPLICATION., 2005, , 105-131.

#	Article	IF	CITATIONS
127	Post radiofrequency ablation assessment of colorectal cancer liver metastases—does post ablation biopsy really matter?. Translational Cancer Research, 2016, 5, S411-S414.	1.0	0
128	Individual nanobubbles detection using acoustic based flow cytometry. , 2019, , .		0
129	Effects of shell-integrated Sudan Black dye on the acoustic activity and ultrasound imaging properties of lipid-shelled nanoscale ultrasound contrast agents. Journal of Biomedical Optics, 2022, 27, .	2.6	Ο